



**HAL**  
open science

## Priority-based data collection for UAV-aided Mobile Sensor Network

Xiaoyan Ma, Tianyi Liu, Song Liu, Rahim Kacimi, Riadh Dhaou

► **To cite this version:**

Xiaoyan Ma, Tianyi Liu, Song Liu, Rahim Kacimi, Riadh Dhaou. Priority-based data collection for UAV-aided Mobile Sensor Network. *Sensors*, inPress, pp.1-24. 10.3390/s20113034 . hal-02617533

**HAL Id: hal-02617533**

**<https://hal.science/hal-02617533>**

Submitted on 25 May 2020

**HAL** is a multi-disciplinary open access archive for the deposit and dissemination of scientific research documents, whether they are published or not. The documents may come from teaching and research institutions in France or abroad, or from public or private research centers.

L'archive ouverte pluridisciplinaire **HAL**, est destinée au dépôt et à la diffusion de documents scientifiques de niveau recherche, publiés ou non, émanant des établissements d'enseignement et de recherche français ou étrangers, des laboratoires publics ou privés.

Article

# Priority-based data collection for UAV-aided Mobile Sensor Network

Xiaoyan MA <sup>1</sup> , Tianyi LIU <sup>2,\*</sup>, Song LIU<sup>1</sup>, Rahim KACIMI <sup>3</sup> and Riadh DHAOU <sup>4</sup>

<sup>1</sup> College of Architecture and Urban Planning, Tongji University, Shanghai 200092, China; xiaoyan.ma@enseeiht.fr, liusong5@tongji.edu.cn

<sup>2</sup> School of Aerospace Engineering and Applied Mechanics, Tongji University, Shanghai 200092, China; tianyi.liu@tongji.edu.cn

<sup>3</sup> IRIT-UPS, University of Toulouse 31062, France; rahim.kacimi@irit.fr

<sup>4</sup> IRIT-ENSEEIH, University of Toulouse 31071, France; riadh.dhaou@enseeiht.fr

\* Correspondence: tianyi.liu@tongji.edu.cn

Version May 24, 2020 submitted to Sensors

**Abstract:** In this work, we study data collection in multiple unmanned aerial vehicle (UAV) aided mobile wireless sensor networks (WSNs). The network topology is changing due to the mobility of the UAVs and the sensor nodes, the design of efficient data collection protocols is a major concern. We address such high dynamic network and propose two mechanisms: prioritized-based contact-duration frame selection mechanism (called PCdFS mechanism), and prioritized-based multiple contact-duration frame selection mechanism (called PMCdFS mechanism) to build collision-free scheduling and balance the nodes between the multi-UAV respectively. Based on the two mechanisms, we proposed a *Balance algorithm* to conduct the collision-free communication between the mobile nodes and the multi-UAVs. Two key design ideas for *Balance algorithm* are: (a) no need of higher priority for those nodes that have lower transmission rate between them and the UAV and (b) improve the communication opportunity for those nodes that have shorter contact duration with the UAVs. We demonstrate the performance of proposed algorithms through extensive simulations, and real experiments. These experiments using 15 mobile nodes at a path with 10 intersections and 1 island, presents that the network fairness is efficiently enhanced. We also confirm the applicability of proposed algorithms in a challenging and realistic scenario through numerous experiments on a path in Tongji campus in Shanghai, China.

**Keywords:** Wireless sensor networks, Multiple unmanned aerial vehicles, Mobile nodes, Data Collection, Collision-free

## 1. Introduction

Unmanned Aerial Vehicles-aided wireless sensor networks (UAV-aided WSN) have gained more and more interest due to its widely applications in monitoring, surveillance, and exploring in healthcare, agriculture, industry, and military [1–5]. Among UAVs' applications, one of the key functions is the data collection [6–11]. These works focus on deterministic topology where the nodes are deployed statically, and the locations of the sensors are known. The data collection issues addressed on dynamic topology, which are usually used in applications such as maritime detection, traffic surveillance, and wilderness rescuing where the targets are moving and no static sensors are deployed in advance, are seldom covered.

The main difference between the static network and mobile network are: *the transmission opportunities for nodes within the coverage of the UAV are different*. In static case, all covered nodes are static, the relative velocity ( $v_r$ ) between the nodes and the UAV are the same. Thus, the contact

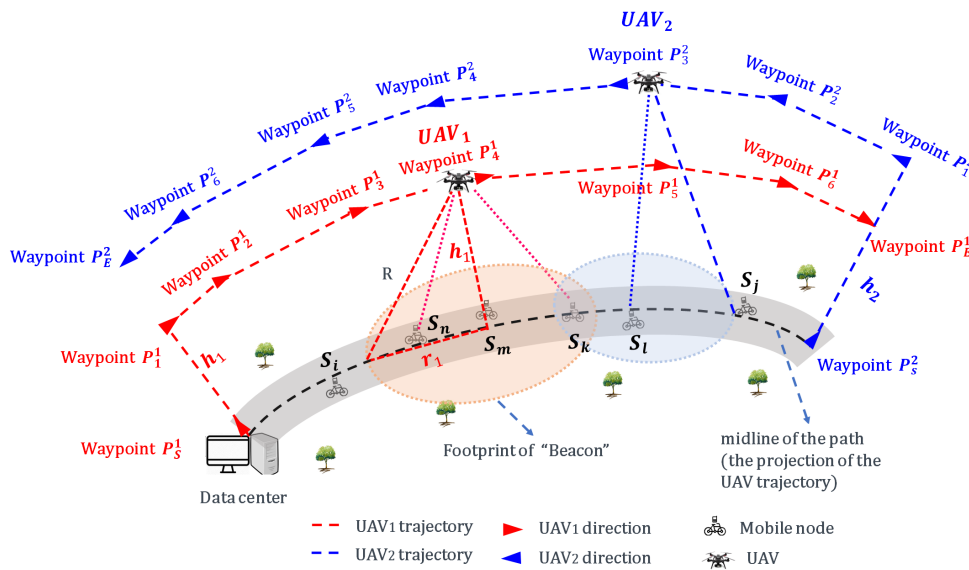


**Figure 1.** An illustration of the UAV-aided data collection for a mobile wireless sensor network. The exemplar trajectory of the  $UAV_1$  is shown as: Waypoint  $P_5^1 \rightarrow$  Waypoint  $P_1^1 \rightarrow$  Waypoint  $P_2^1 \rightarrow$  Waypoint  $P_3^1 \rightarrow$  Waypoint  $P_4^1 \rightarrow$  Waypoint  $P_5^1 \rightarrow$  Waypoint  $P_6^1 \rightarrow$  Waypoint  $P_E^1$ .

31 durations (CD) between them with the UAV depend on the relative distance ( $d_r$ ) between them  
 32 ( $CD = \frac{d_r}{v_r}$ , see [12,13] for more details). The relative distances almost have no difference if the UAV fly  
 33 at a higher height. However, in mobile case, when the nodes move at different velocities, the CD are  
 34 different greatly even the relative distance is the same. Intuitively, the shorter the CD between them,  
 35 the smaller the opportunities for the mobile node to communicate with the UAV. When the CD is very  
 36 short, the mobile node may have no opportunity to communicate with the UAV if no attention is paid  
 37 on the CD between it with the UAV. Thus, a contact-duration-based data collection algorithm should  
 38 be design for such context despite a large array of existing data collection algorithms (see Section 2.  
 39 related works) on UAV-aided static WSNs.

40 The impact factors of the CD between mobile nodes and the UAV include two aspects: (a)  
 41 the relative distance between the sensor and the UAV, and (b) the relative velocity between them.  
 42 Priority-based Frame Selection (PFS) [14,15] is a one-hop mechanism based on the relative distance  
 43 according which the nodes are divided into different priority groups. Communications are conducted  
 44 from higher to lower priorities. In [16], the authors propose a multi-hop highest velocity opportunistic  
 45 algorithm which is based on relative velocity between mobile nodes and the UAV. The ones that have  
 46 higher velocity have longer CD with the UAV therefore were selected as forwarded nodes. In our  
 47 previous work [12,13], we studied the data collection maximization issues in a *single* UAV-aided mobile  
 48 WSN where the pre-defined path is a straight path without comparison with existing works and real  
 49 experiments. The curve path and multi-UAVs aspects are also not covered in the previous work. Thus,  
 50 a large room for enhancing the network performance still exists.

51 In this work, we focus on multi-UAV aided mobile WSN, Figure 1, where the nodes are deployed  
 52 on mobile bicycles and move along a pre-defined curve path. Considering that, in the context of  
 53 the nodes move along a path, two UAVs are enough to cover all mobile nodes when (as in Figure 1)  
 54  $UAV_1$  take-off from the original point of the path and fly along the path,  $UAV_2$  take-off from the end  
 55 point of the path and fly along the path. Data collection issues in such context contain two aspects.  
 56 End-to-end Data collection is a very [complex] problem. In this paper, we focus on the access link.  
 57 As the literature, on this kind of link between the sensors and the UAV [6,7], still does not propose  
 58 efficient solutions. The access link suffers from synchronization problem due to the high dynamic  
 59 network, the coordination between the mobile nodes and the multi-UAVs. Providing the opportunity  
 60 of communication to the nodes that have very short duration with the UAVs reduces the congestion

61 risk. On the other side, an extensive literature can be referred to, on the second link, on the backhaul  
62 link, between the UAVs and gateways [17]. The second link is also challenging on several levels such  
63 as the data security, the security of UAVs, and the dimensioning of the backhaul. In our previous work  
64 [18,19], we focused on the backhaul link with satellite system. The proposed algorithms on mobile  
65 mules, in [18,19] are applicable for UAV-aided sensor networks. Moreover, because that the collected  
66 data (considering the value of data and distinguish the data collected from each sensor) could be stored  
67 in SD cards embedded on the UAV, thus, in this work, we focus on the access link. The data collection  
68 optimization objectives in such context include two aspects: (i) maximizing the number of collected  
69 packets, and (ii) maximizing the number of nodes that successfully send at least one packet during the  
70 collection period. Our main purpose is to jointly maximize the two aspects through formulating the  
71 dynamic parameters. Our main contributions are summarized as follows:

- 72 • We study the impact of dynamic parameters, including the speed and flying height of UAV, the  
73 sensor speed, network size, and different priority areas. We mathematically formulate the data  
74 collection issue into the optimization with the objective of maximizing the number of collected  
75 packets and the number of sensors that successfully send packets to the UAVs.
- 76 • Based on the dynamic parameters, we adopt time discrete mechanism and propose a  
77 Prioritized-based Multiple Contact-duration Frame Selection algorithm (named PMCdFS  
78 algorithm). PMCdFS algorithm is used for the balancing between the nodes (that are within the  
79 range of multi-UAVs at the same time) and multi-UAVs.
- 80 • We improve the contact duration mechanism in our previous work (see [12,13] for more details)  
81 with the Prioritized Frame Selection (PFS) mechanism (see [14,15] for more details) and propose  
82 Prioritized-based Contact-duration Frame Selection algorithm (named PCdFS algorithm). *PCdFS*  
83 *algorithm* is a one-hop and slotted mechanism which is used to allocate the time-slot for the nodes  
84 that covered only by one of the UAVs.
- 85 • We propose a *Balance algorithm* to solve the collision between the nodes and UAVs so as to  
86 optimize the aforementioned data collection performance.
- 87 • Through extensive simulations, and real experiments, we examine the effectiveness of the  
88 proposed algorithms, and compare it with existing algorithm under different configurations.

89 The reminder of this paper is organized as follows: In the next section, we discuss previous  
90 related work. Section 3 presents the system model and the problems formulated. Section 4 present the  
91 proposed algorithms. Section 5 evaluated the proposed algorithms through extensive simulations and  
92 real experiments. Section 6 concludes this paper and gives some future work suggestions.

## 93 2. Related Works

94 There exists an extensive array of research on data collection in UAV-aided WSN with different  
95 objectives ranging from completion time minimization [20], power controlling [21], trajectory distance  
96 minimizing [22] to energy consumption minimization [23,24]. We classify these existing data collection  
97 algorithms by two criteria: (i) Static or mobile nodes, and (ii) sensors are deployed along a path or  
98 deployed within an interesting area. In (i), algorithms are differentiated by whether the sensors mobile  
99 or not because the dynamic parameters brought by the movement of nodes in the network structure  
100 have much greater impact on the system performance. In (ii), algorithms are differentiated by whether  
101 the nodes deployed along a path or not. The nodes deployed along a given path [12,13,25,26] so the  
102 UAV trajectory planning has very little impact on the network performance.

103 (i): Data collection algorithms addressed on **mobile** nodes. There are many works on studying  
104 how to collected data from WSN. The authors in [4,9,27–29] review these works. According to the  
105 [4,9,27–29], most of these algorithms only based on mobile sink or only focused on mobile sensors.  
106 In our previous works [12,13,16], we studied how to use UAV to collect data from mobile nodes  
107 based on an assumption that both the nodes and the UAV move along a straight path with constant  
108 speeds. Generally case that both the UAV and the nodes move at a curve path are not considered.

**Table 1.** Summary of Related Work.

Ref.	Sensor status	$N_{uav}$	Descriptions
[6]	Static deployed	1	Through UAV trajectory planning to achieve timely data collection from IoT devices where the data has deadlines and needs to be sent before the data loses its meaning or becomes irrelevant.
[7]	Static deployed	1	Considering the age of information, characterized by the data uploading time and the time elapsed since the UAV leaves a node, when designing the UAV trajectory.
[11]	Static deployed	1	To extend the lifetime of the network through charging for the UAV in the air.
[14, 15]	Static deployed	1	The authors divided the interesting area into different priority groups, and the data communication conducted from higher to lower priorities (PFS mechanism). Based on PFS, the authors proposed a MAC protocols for UAV-aided WSN.
[24]	Static deployed	1	the authors through optimizing the trajectory of a rotary-wing UAV to collect data with an objective of minimizing the maximum energy consumption of all devices.
[25]	Static deployed	1	To minimize the flight time, and jointly optimize the transmit power of nodes, the UAV speed and the transmission intervals.
[30]	Static deployed	1	To optimize the UAV's trajectory, height, velocity, and data links with ground users so as to minimize the total mission time.
[31]	Static deployed	1	To minimize the energy consumption of the system through optimizing the UAV's trajectory and devices' transmission schedule, while ensuring the reliability of data collection and required 3-D positioning performance.
[32]	Static deployed	1	To maximize the minimum average data collection rate from all nodes subject to a prescribed reliability constraint for each node by jointly optimizing the UAV communication scheduling and three-dimensional trajectory.
[33]	Static deployed	1	To minimize the maximum delay of all ground users through jointly optimizing the offloading ratio, the users' scheduling variables, and UAV's trajectory.
[34]	Static deployed	1	To maximize the minimum received energy of ground users by optimizing the trajectory of the UAV. They first presented the globally optimal one-dimensional (1D) trajectory solution to the minimum received energy maximization problem.
[20]	Static deployed	Multiple	Minimize the maximum mission completion time through jointly optimize the wake-up scheduling and association for sensors, the UAV trajectory, while ensuring that each node can successfully upload the targeting amount of data with a given energy budget.
[35]	Static deployed	Multiple	To maximize the data collection utility by jointly optimizing the communication scheduling and trajectory for all UAVs.
[36]	Static deployed	Multiple	The authors proposed a risk-aware trajectory planning algorithm for multi-UAVs for urban applications.
[37]	Static deployed	Multiple	To minimize the mission completion time of the UAVs through designing the UAV's trajectory, and meanwhile, they guaranteed that each ground user can successfully recover the file.
[38]	Static deployed	Multiple	To maximize the minimum throughput of ground users through optimizing the trajectory for each UAV.
[39]	Static deployed	Multiple	To minimize the mission time by planning the trajectory of each UAV, while satisfying the time requirements.
[40]	Static deployed	Multiple	Use nested Markov chains to analyze the probability for successful data transmission, and propose a sense-and-send mechanism for real-time sensing missions, and a multi-UAVs based Q-learning algorithm for decentralized UAV trajectory planning.
this paper	Mobile	Multiple	Collect data from mobile nodes through balancing the different contact durations between mobile nodes, and multi-UAVs.

109 Numerous of research have been done on **static** deployed networks [6,7,11,14,15,20,24,25,30–35,35–40].  
 110 (see Table 1 for the key focuses for them, and the key difference of our proposed algorithms from  
 111 existing algorithms).

112 (ii): Most of aforementioned data collection algorithms can also be classify according to the  
 113 deployed status of the nodes. Authors in [12,13,16,25,34] studied how to use UAV to collect data  
 114 from nodes that deployed along a **straight path**. Especially in [25], the nodes deployed on a straight  
 115 line, and the UAV fly over this line to collect data from nodes. In such context, the trajectory of the  
 116 UAV dependent on the path (or line) and it has light impact on the performance if the path is longer  
 117 enough. For instance, in [25], the authors aim to minimize the flight time through jointly optimizing  
 118 the transmit power of nodes, the UAV speed and the transmission intervals. For the case that nodes  
 119 are deployed within an **interesting area**, one of the main issues is to plan the UAV's trajectory so  
 120 as to enhance the network performance. Numerous research have been done on the UAV trajectory  
 121 planning issues [6,7,20,24,30–35,35–40]. These works are different in the optimization method and  
 122 objective function because of different scenarios. They are mainly classified into two types: *single-UAV*  
 123 *trajectory planning* [6,7,24,30–34] and *multi-UAV trajectory planning* [20,35–40].

124 *Single-UAV trajectory planning*. Authors in [33] use a UAV for the mobile edge computing system.  
 125 They minimize the maximum delay of all ground users through jointly optimizing the offloading ratio,  
 126 the users' scheduling variables, and UAV's trajectory. While in [24], the authors aim to minimize the  
 127 maximum energy consumption through optimizing the trajectory of a rotary-wing UAV. And in [6], the  
 128 authors utilize a UAV to collect data from IoT devices with each has limited buffer size and target data  
 129 upload deadline. In this study, the data should be transmitted before it loses its meaning or becomes  
 130 irrelevant. To maximize the number of served IoT devices, they jointly optimizing the radio resource  
 131 allocation and the UAV's trajectory.

132 *Multi-UAV trajectory planning*. In [38], multi-UAVs used as mobile base stations to provide service  
 133 for ground users. They aim to maximize the minimum throughput of ground users through optimizing  
 134 the trajectory for each UAV. And in [20], they employ multi-UAVs to collect data from nodes. Through  
 135 jointly optimizing the trajectories of UAVs, wake-up association and scheduling for sensors, they  
 136 minimize the maximum mission completion time of all UAVs. In [37], the authors studied a multiple  
 137 casting network utilizing the UAV to send files to all ground users. They aim to minimize the mission  
 138 completion time of the UAVs through designing the UAV's trajectory. Meanwhile, the proposed  
 139 algorithms guarantee that each ground user can successfully recover the file. In urban applications,  
 140 the authors proposed a risk-aware trajectory planning algorithm [36] for multi-UAVs. Under the same  
 141 test scenarios, authors in [39] aim to minimize the mission time by planning the trajectory of each UAV.  
 142 In [40], the scholars exploit the nested Markov chains to analyze the probability for successful data  
 143 transmission. They propose a sense-and-send mechanism [40] for real-time sensing missions, and a  
 144 multi-UAVs enabled Q-learning algorithm for decentralized UAV trajectory planning.

145 *Other cases*. In [11], they use a single UAV to collect data from harsh terrains. Due to the large  
 146 scale of the detection area, the network has a high demand for power. They adopted a rechargeable  
 147 mechanism to extend the lifetime of the UAV so as to enhance the collection period. The PFS mechanism  
 148 in [14,15] is based on the nodes' positions for the data collection in single-UAV aided static sensor  
 149 networks. The nodes are divided into different priority groups according two steps: (i). increasing  
 150 group and decreasing group (Figure 2). The nodes that within the decreasing group was given higher  
 151 priority than the ones within increasing group. (ii). For each group in (i), the nodes were divided into  
 152 sub-group according to which power level does it belong to. The sets of nodes that within "power level  
 153 1" in increasing group and in decreasing group are denoted by  $S_{a,I}^1$  and  $S_{a,D}^1$ , respectively. The priority  
 154 values for nodes within  $S_{a,I}^1$  and  $S_{a,D}^1$  are denoted by  $P_{a,I}^1$  and  $P_{a,D}^1$ , respectively. The authors give high  
 155 priority to those nodes that are within high power level (Figure 2), and applied opposite actions to  
 156 the increasing and decreasing groups: (a) In increasing group, the nodes within high power level was  
 157 given high priority value; (b) In decreasing group, the nodes within lower power level were given

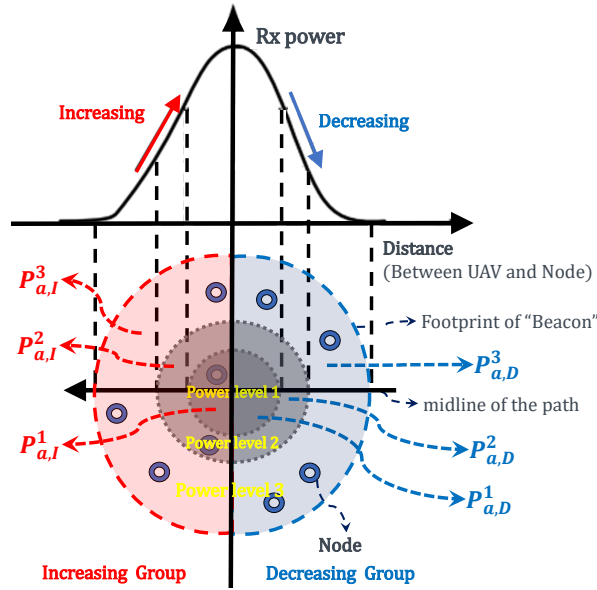


Figure 2. The Priority Frame Selection (PFS) mechanism.

158 high priority. After these actions, almost all nodes that are at the best channel conditions have been  
 159 considered.

160 Although much research have been done on data collection, there is still room to enhance  
 161 the network performance through balancing the dynamic parameters in first link in mobile sensor  
 162 networks.

### 163 3. System Model and Problem Formulation

#### 164 3.1. System Model

165 This paper considers a UAV-assisted mobile sensor network which has  $N$  mobile bicycles with  
 166 each equipped a sensor, and  $M$  UAVs with each equipped a sensor (as illustrated in Figure 1, where  $M$   
 167  $= 2$ ).  $\mathbb{S} = \{S_1, S_2, \dots, S_N\}$  is the set of mobile sensors.  $N$  nodes move along a pre-defined path (path  
 168 length is denoted as  $L$ ) with each has a speed  $v_i$ . The UAV  $U_i$  is dispatched to collect data from mobile  
 169 sensors at a given height  $h_i$  and speed  $v_u^i$  along a predefined trajectory (Figure 1).

170 The trajectory consists of a few number of line segments that contain the "Waypoint Start" and  
 171 "Waypoint End" (e.g., in Figure 1, "Waypoint  $P_S^i$ " and "Waypoint  $P_E^i$ " in the trajectory of  $UAV_i$ ,  $i$   
 172  $= 1, 2$ ), and  $k$  intermediate waypoints (e.g., in Figure 1, "Waypoint  $P_1^i$ ", "Waypoint  $P_2^i$ ", "Waypoint  
 173  $P_3^i$ ", "Waypoint  $P_4^i$ ", "Waypoint  $P_5^i$ " and "Waypoint  $P_6^i$ " in the trajectory of  $UAV_i$ ,  $i = 1, 2$ ). Let  $\mathbb{P}_i =$   
 174  $\{P_S^i, P_1^i, P_2^i, \dots, P_k^i, P_E^i\}$  denote the set of all waypoints of  $UAV_i$ . The coordinates for each waypoint  $P_m^i$   
 175 is denoted by  $P_m^i(x_m^i, y_m^i, h_i)$ . The UAV's flight time between any two waypoints  $P_m^i$  and  $P_n^i$  is given by,

$$\lambda_{m,n}^i = \frac{\|P_m^i - P_n^i\|}{v_u^i}, \quad P_m^i, P_n^i \in \mathbb{P}_i. \quad (1)$$

The collection period of the  $UAV_i$  is the duration from "Waypoint  $P_1^i$ " to the "Waypoint  $P_E^i$ ". And,  
 it is denoted by  $T_i$ ,

$$T_i = \sum_{m=1}^{k-1} \lambda_{m,m+1}^i + \lambda_{k,E}^i. \quad (2)$$

The trajectory length for  $UAV_i$  is,

$$L_i = \sum_{m=1}^{k-1} \|P_{m+1}^i - P_m^i\| + \|P_E^i - P_k^i\|. \quad (3)$$

**Table 2.** Major notations used in this article.

Parameters	Descriptions
$N$	Network size;
$M$	The number of UAVs;
$UAV_i$	The $i^{th}$ UAV;
$\mathbb{S}$	The sensors set;
$\mathbb{S}_{kB}^i$	The sensors set that within the range of $UAV_i$ in $t_k$ ;
$\mathbb{S}_{kB}^{i,o}$	The sensors set that only within the range of $UAV_i$ in $t_k$ ;
$\mathbb{S}_{kB}^{i,j}$	The sensors set that within the range of both $UAV_i$ and $UAV_j$ in $t_k$ ;
$\mathbb{U}$	The UAVs set;
$T_i$	The collection period of the $UAV_i$ ;
$h_i$	The fly height of the $UAV_i$ ;
$L$	The path length;
$L_i$	The length of the trajectory of $UAV_i$ ;
$N_{ts}$	The number of time slots;
$\mathbb{T}$	The set of time-slots;
$\alpha$	The duration of one time-slot;
$P_m^i, P_S^i, P_E^i$	The " $m^{th}$ ", the "start", and the "end" way points of the $UAV_i$ respectively;
$\mathbb{P}_i$	The set of way points for $UAV_i$ ;
$\lambda_{m,n}^i$	The UAV's flight time between any two waypoints $P_m^i$ and $P_n^i$ of $UAV_i$ ;
$\mathbb{F}$	The set of nodes that send at least one packet in collection period;
$t_B$	The duration between adjacent two "Beacon";
$N_{ts,a}(i, j, k)$	A matrix where value is "0" and "1". $N_{ts,a}(i, j, k) = 1$ implies in $t_k$ , the $UAV_i$ will communicate with $S_j$ , and othwise it is "0";
$\sigma_{ijk}$	Boolean function. $\sigma_{ijk} = 1$ implies that the $UAV_i$ successfully collect data from $S_j$ in $t_k$ ;
$N_{t,a}^i$	The number of time slots that sensor $S_i$ ( $S_i \in \mathbb{S}$ ) was allocated in time $T$ ;
$N_p$	The total number of collected packets;
$N_{node}$	The number of nodes that successfully send at least one packets.

176 Generally, in a given path, the coordinates (x-axis and y-axis) of the waypoints for the UAVs are  
 177 the same except the height (z-axis). For instance, the point  $(x_m^i, y_m^i, h_j)$  is one of the waypoints for  
 178  $UAV_j$  (i.e.,  $P_m^j(x_m^i, y_m^i, h_j) \in \mathbb{P}_j$ ) if  $P_m^i(x_m^i, y_m^i, h_i) \in \mathbb{P}_i$ . Thus, we have  $L_i = L_j$ . Intuitively, the straighter  
 179 the pre-defined path, the smaller the  $\Delta L$  ( $\Delta L = |L - L_i|$ ). The larger the number of waypoints, the  
 180 smaller the  $\Delta L$ . The major notations used in this work are defined in Table 2.

181 To well present the impact of the dynamic parameters on the system, we using homogeneous  
 182 UAVs ( $v_u^i = v$ ) to reduce the influence brought by UAVs' speeds. Accordingly, the collecting period is  
 183 denoted by  $T$ , and  $T = T_i$ .

### 184 3.2. Discrete Time mechanism

185 Considering the waypoint selection and beacon sending, we introduce a discrete-time mechanism  
 186 where the collecting period  $T$  is divided into  $N_{ts}$  time-slots with each lasting  $\alpha$  time units,  $N_{ts} = \lfloor \frac{T}{\alpha} \rfloor$ ,  
 187 where  $\lfloor \cdot \rfloor$  is the rounding down function. It is assumed that the time-slots are indexed as  $1, 2, \dots, N_{ts}$ ,  
 188 and  $\mathbb{T} = \{t_1, t_2, \dots, t_{N_{ts}}\}$  (Figure 3). It is worth note that, in each time slot, a sensor could communicate  
 189 only with one UAV. For example, in  $t_k$ ,  $S_i$  communicate with  $UAV_m$ , and  $S_j$  communicate with  $UAV_n$   
 190 ( $i \neq j$  and  $m \neq n$ ).

191 From Figure 1, the nodes that are covered by the  $UAV_i$  and deployed nearly complete to  
 192 communicate with the  $UAV_i$ . For instance,  $S_m, S_n, S_k$  in Figure 1 complete to communicate with  
 193 the  $UAV_1$ . Meanwhile, there are more than one UAV within the range of one node. For example,  $S_k$  in  
 194 Figure 1 with the range of both  $UAV_1$  and  $UAV_2$ . The  $S_k$  should choice one from them to send packets.  
 195 Hence, how to balance the communication between nodes and the UAVs so as to maximize the data  
 196 collection is a challenging task.

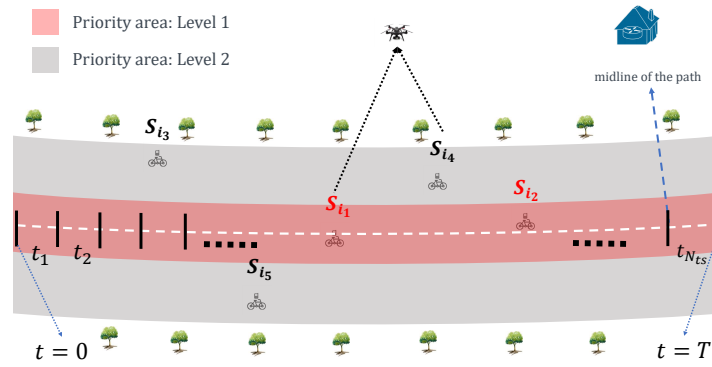


**Figure 3.** An illustration of studied scenario.

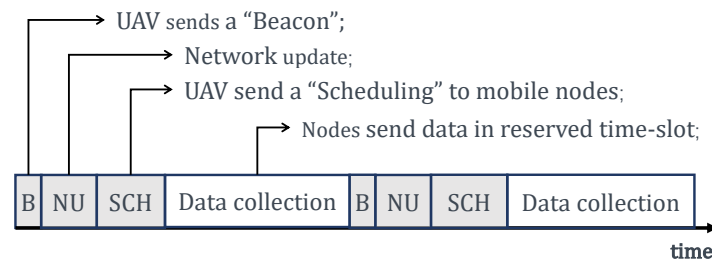


**Figure 4.** The procedure of allocating.

### 197 3.3. Data Collection Protocols Using UAV

198 In this paper, we present a distributed method for the data collection issues in UAV-aided mobile  
 199 sensor network as follows. The collection period  $T$  is divided into  $N_{ts}$  time slots. At the beginning of  
 200 every time slot (Figure 4), UAV sends a "Beacon" message to tell the mobile nodes that UAV is coming.  
 201 The "Beacon" includes the UAV's information, e.g., the fly height, the speed, etc. The new comers send  
 202 a *JOIN* message which includes the sensors' information to the UAV to update the network topology.  
 203 The UAV judges whether the nodes are within its range or not according to these messages. Then, it  
 204 calculates the contact duration, the relative distance, and the potential time slots for each node that  
 205 successfully send *JOIN* message. According to the time slot allocation algorithms that we proposed in  
 206 section 4, the UAV provides a scheduling for the covered sensors, and broadcasts them a "Scheduling"  
 207 message which contains the assignment of the time-slots. Having received the "Scheduling" message,  
 208 every sensor transmits its data in its own time slots.

#### 209 3.3.1. Collecting packets

210 Allocating the  $N_{ts}$  time slots to individual mobile sensors under proposed mechanism is equivalent  
 211 to maximizing the usage of time slots. Let,

$$N_{ts,a}(i, j, k) = \begin{cases} 1 & \text{UAV}_i \text{ communicate with } S_j \text{ in } t_k, \\ 0 & \text{otherwise.} \end{cases}$$

The data collection maximization problem is to maximize the number of collected packets,  $N_p$ ,

$$N_p = \sum_{i=1}^M \sum_{j=1}^N \sum_{k=1}^{N_{ts}} N_{ts,a}(i, j, k) \cdot \sigma_{ijk} \cdot D_r \cdot \alpha. \quad (4)$$

212 where  $D_r$  is the transmission rate, and

$$\sigma_{ijk} = \begin{cases} 1 & \text{successfully transmission,} \\ 0 & \text{otherwise.} \end{cases}$$

213 Our objective is to balance the communication between the two UAVs and  $N$  mobile nodes to  
214 maximize the overall data collection utility. Therefore, the optimization problem can be formulated as,

$$\mathcal{P}_1 : \max_{S_j \in \mathbb{S}, t_k \in \mathbb{T}} \{N_p\}, \quad (5)$$

$$\text{s.t.} \quad \sum_{k=1}^{N_{ts}} N_{ts,a}(i, j, k) \leq N_{ts}, \forall i, j, \quad (6)$$

$$\sum_{j=1}^N N_{ts,a}(i, j, k) \leq N, \forall i, k, \quad (7)$$

$$\sum_{i=1}^M N_{ts,a}(i, j, k) \leq M, \forall j, k, \quad (8)$$

$$\sum_{i=1}^M \sum_{j=1}^N \sum_{k=1}^{N_{ts}} N_{ts,a}(i, j, k) \leq M \cdot N_{ts}, \forall i, j. \quad (9)$$

215 Constraints (6), (7), (8) imply that, in a given time-slot, a UAV choice only one node to collect data,  
216 and one node select only one UAV to send data. Constraints (9) ensures that, in a given time-slot, no  
217 more than two communications happen between UAVs and mobile nodes.

218 3.3.2. The number of nodes that successfully send packets to the UAV

219 During the communicating between the UAVs and mobile nodes, the sensors transmission state  
220 contains: have no opportunity to send packets, have an opportunity to send but fail to transmit, and  
221 successfully send data to the UAVs. The larger number of nodes ( $N_{node}$ ) that successfully transmit  
222 packets, the higher the system performance. Thus, to enhancing the number of nodes that successfully  
223 send data to the UAVs is one of the key point in designing data collection algorithms.

224 Let matrix  $I_{M \times N \times N_{ts}}$  is given by,

$$I_{ijk} = N_{ts,a}(i, j, k) \cdot \sigma_{ijk} \cdot i, \quad UAV_i \in \mathbb{U}, S_j \in \mathbb{S} \text{ and } t_k \in \mathbb{T}.$$

225 Then, the elements in matrix  $I$  is the node ID. Then, we can obtain the number of nodes that  
226 successfully transmit at least one packet,

$$N_{node} \triangleq \text{Hist}(I). \quad (10)$$

227 Where "Hist" is used to calculated the number of different elements in the  $I$  matrix. The  $N_{node}$   
228 maximization problem can be regarded as the formulated problem,

$$\mathcal{P}_2 : \max_{S_j \in \mathbb{S}, t_k \in \mathbb{T}} \{N_{node}\}, \quad (11)$$

$$s.t. \quad \sum_{k=1}^{N_{ts}} N_{ts,a}(i, j, k) \leq N_{ts}, \forall i, j, \quad (12)$$

$$\sum_{j=1}^N N_{ts,a}(i, j, k) \leq N, \forall i, k, \quad (13)$$

$$\sum_{i=1}^M N_{ts,a}(i, j, k) \leq M, \forall j, k, \quad (14)$$

$$\sum_{i=1}^M \sum_{j=1}^N \sum_{k=1}^{N_{ts}} N_{ts,a}(i, j, k) \leq M \cdot N_{ts}, \forall i, j. \quad (15)$$

229 When  $i = 1$  (single-UAV enabled sensor network), it is a classical NP-hard problem that we have  
 230 studied in [12,13]. When  $i = 2$  (multi-UAV enabled sensor network), this problem is also a NP-hard  
 231 combinatorial maximization problem [41]: under the given conditions, its objective is to select items  
 232 which have unique weight and value to maximize the total value.

#### 233 4. Proposed Algorithms

234 In this section, we study how to balance the communication between multi-UAVs and mobile  
 235 nodes, and we propose a *balance mechanism*. For the two cases, multiple nodes within the range  
 236 of both two UAVs and multiple nodes only with the range of only one UAV, we propose two  
 237 algorithms: Priority-based Contact-duration Frame Selection (PCdFS) (section 4.2) and Priority-based  
 238 Multiple-Contact-duration Frame Selection (PMCDFS) (section 4.3) algorithms.

##### 239 4.1. Balance Algorithm between UAVs and Mobile Nodes

240 In a given time slot  $t_k$  ( $t_k \in \mathbb{T}$ ), there are multiple nodes within the range of the UAV. The nodes  
 241 that are potentially for  $UAV_1$  and  $UAV_2$  are denoted by  $\mathbb{S}_{kB}^1$  and  $\mathbb{S}_{kB}^2$  respectively. When  $\mathbb{S}_{kB}^1 \cap \mathbb{S}_{kB}^2$   
 242  $= \emptyset$ , there is no node within the range of the  $UAV_1$  and  $UAV_2$  at the same time. In this case, we  
 243 propose Priority-based Contact-duration Frame Selection (PCdFS) Mechanism (see section 4.2 for more  
 244 details) to balance the communications between  $\mathbb{S}_{kB}^1$  and  $UAV_1$ ,  $\mathbb{S}_{kB}^2$  and  $UAV_2$  respectively. When  
 245  $\mathbb{S}_{kB}^1 \cap \mathbb{S}_{kB}^2 \neq \emptyset$ , and  $\mathbb{S}_{kB}^{1,2} \triangleq \mathbb{S}_{kB}^1 \cap \mathbb{S}_{kB}^2$ . Then,

$$\mathbb{S}_{kB}^{1,o} \triangleq \mathbb{S}_{kB}^1 - \mathbb{S}_{kB}^{1,2}, \quad (16)$$

$$\mathbb{S}_{kB}^{2,o} \triangleq \mathbb{S}_{kB}^2 - \mathbb{S}_{kB}^{1,2}, \quad (17)$$

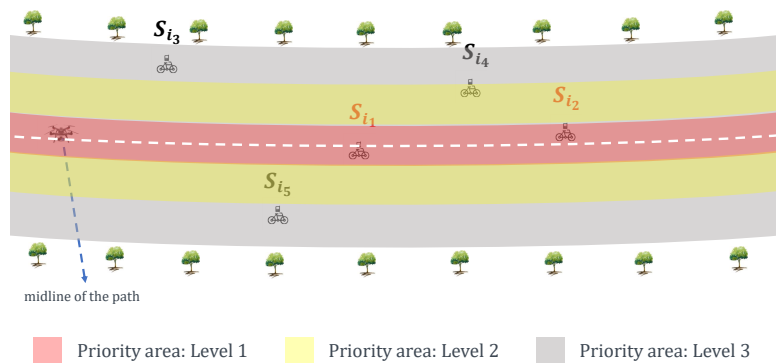


Figure 5. Priority areas.

**Algorithm 1** Balance Algorithm**Input:** Initial deployed information of nodes and UAVs**Output:**  $N_p, N_{node}$ 


---

```

1:  $N_p = N_{node} = 0, k = 1, T_{now} = 0;$ 
2: Step 1. Synchronization;
3: UAV sends  $k - th$  'Beacon' message;
4: Network update, obtain the  $\mathbb{S}_{k_B}^1$  and  $\mathbb{S}_{k_B}^2$ ;
5: Step 2. Data Communication;
6: while  $T_{now} < T$  do
7:   Let  $\mathbb{S}_{k_B}^{1,2} \triangleq \mathbb{S}_{k_B}^1 \cap \mathbb{S}_{k_B}^2, \mathbb{S}_{k_B}^{1,o} \triangleq \mathbb{S}_{k_B}^1 - \mathbb{S}_{k_B}^{1,2}$ , and  $\mathbb{S}_{k_B}^{2,o} \triangleq \mathbb{S}_{k_B}^2 - \mathbb{S}_{k_B}^{1,2}$ ;
8:   if  $\mathbb{S}_{k_B}^{1,2} = \emptyset$  then
9:     Apply PCdFS mechanism (Algorithm 2) to balance the communication between  $\mathbb{S}_{k_B}^{1,o}$  and
       UAV1,  $\mathbb{S}_{k_B}^{2,o}$  and UAV2 respectively;
10:   else
11:     Apply PMCdFS algorithm (Algorithm 3) for the balancing between mobile nodes in  $\mathbb{S}_{k_B}^{1,2}$ 
       and multi-UAVs, and obtain  $\mathbb{S}_{k_B}^1$  and  $\mathbb{S}_{k_B}^2$  through PMCdFS algorithm;
12:     Apply PCdFS mechanism (Algorithm 2) to balance the communication between  $\mathbb{S}_{k_B}^{1,o}$  and
       UAV1,  $\mathbb{S}_{k_B}^{2,o}$  and UAV2 respectively;
13:   end if
14:   Update  $T_{now}, k, N_p$  and  $N_{node}$ ;
15: end while
16: return  $N_p$  and  $N_{node}$ ;

```

---

246  $\mathbb{S}_{k_B}^{1,o}$  and  $\mathbb{S}_{k_B}^{2,o}$  are denoted the sensors set that only within the range of the UAV<sub>1</sub> and  
247 UAV<sub>2</sub> respectively. We use PCdFS mechanism to balance the communications between  $\mathbb{S}_{k_B}^{1,o}$   
248 and UAV<sub>1</sub>,  $\mathbb{S}_{k_B}^{2,o}$  and UAV<sub>2</sub> respectively. For the nodes within  $\mathbb{S}_{k_B}^{1,2}$ , we proposed Priority-based  
249 Multiple-Contact-duration Frame Selection (PMCdFS) algorithm to balance between  $|\mathbb{S}_{k_B}^{1,2}|$  mobile  
250 nodes and multi-UAVs. The *Balance Algorithm* is detailed in Algorithm 1.

251 **4.2. Priority-based Contact-duration Frame Selection Mechanism**

252 In Priority-based Contact-duration Frame Selection (PCdFS) mechanism, the priority areas  
253 division include two steps: (i). Divide the nodes into different groups according to which power level  
254 does them belong to. Take Figure 3 and Figure 5 for example, the nodes were divided into two groups  
255 and three groups, respectively. Figure 3,  $S_{i_1}$  and  $S_{i_2}$  are within the same priority area (level 2),  $S_{i_3}$ ,  $S_{i_4}$   
256 and  $S_{i_5}$  are within level 2. If we take into account more priority levels, e.g., 3 levels as in Figure 5,  $S_{i_1}$   
257 and  $S_{i_2}$  are within level 1,  $S_{i_4}$  is in level 2,  $S_{i_3}$  and  $S_{i_5}$  are in level 3. More levels, more detailed group.  
258 (ii). For each group, the nodes were given different priority value according to their contact duration  
259 with the UAV. The ones that have shorter CD with the UAV were given higher priority values. In,  
260 PCdFS, different nodes were given different priority values except the case that there exist more than  
261 one node have the same CD with the UAV. In PCdFS, it makes the nodes that are facing to a loosing  
262 of the connection with the UAV are highly concerned. In addition, PCdFS provide the nodes within  
263 higher power level to send data exactly at the moment of their good channel condition so as to reduce  
264 the packets loss. The PCdFS algorithm is detailed in Algorithm 2.

**Algorithm 2** PCdFS Algorithm**Input:** Initial deployed information of nodes and UAVs,  $\mathbb{S}_{kB}^1, \mathbb{S}_{kB}^2, N_p, N_{node}$ .**Output:**  $N_p, N_{node}$ 

- 1: **for**  $\forall S_i \in \mathbb{S}_{kB}^1, \forall S_j \in \mathbb{S}_{kB}^2$  **do**
- 2:     Make a judgement for sensor  $S_i$  and  $S_j$ : which priority area does them in;
- 3:     Calculate the *contact duration* between  $S_i$  and the  $UAV_1, S_j$  and the  $UAV_2$ , respectively;
- 4: **end for**
- 5: For  $UAV_1$  (and  $UAV_2$ ),  $t_k$  allocated to the one (e.g.  $S_{i_k}$ , and  $S_{i_k} \in \mathbb{S}_{kB}^1$  for  $UAV_1$ , and  $S_{j_l}, S_{j_l} \in \mathbb{S}_{kB}^2$  for  $UAV_2$ ) which within the higher priority area; When more than one node within the same high priority area,  $t_k$  allocated to the one (e.g.,  $S_{i_k}$  for  $UAV_1$ , and  $S_{j_l}$  for  $UAV_2$ ) which has the shorter contact duration with the UAV.
- 6: In  $t_k, S_{i_k}$  and  $S_{j_l}$  send packets to  $UAV_1$  and  $UAV_2$  respectively;
- 7: Update  $N_p, N_{node}$ ;
- 8: **return**  $N_p$  and  $N_{node}$ ;

## 265 4.3. Priority-based Multiple-Contact-duration Frame Selection Mechanism

266     The Priority-based Multiple-Contact-duration Frame Selection (PMCdFS) algorithm is used to  
 267 balance the communications between the UAVs and nodes when these nodes are within the range of  
 268 the multi-UAVs at the same time. Intuitively, the longer the CD between the nodes and the UAV, the  
 269 higher the opportunity to send packets to the UAV. Thus, it increase the transmission opportunity of  
 270 the node if it was arranged to the UAV which has longer CD between it and the UAV. The PMCdFS is  
 271 detailed in Algorithm 3. Through PMCdFS algorithm, we obtain the sensors set in which all nodes  
 272 only compete to communicate with a single UAV ( $UAV_1$  or  $UAV_2$ ). Then, we apply PCdFS algorithm  
 273 to conduct the communication among them. The proposed algorithms are summarized in Table 3.

274     In the following, we will evaluate the proposed algorithms through different configures, and  
 275 compare our proposed algorithms with the existing algorithm (PFS).

## 276 5. Implementation and Evaluation

277     We implement the algorithms in both simulations and real experiments as following.

**Algorithm 3** PMCdFS Algorithm**Input:** Initial deployed information of nodes and UAVs,  $\mathbb{S}_{kB}^{1,2}, \mathbb{S}_{kB}^1, \mathbb{S}_{kB}^2$ .**Output:**  $\mathbb{S}_{kB}^1$  and  $\mathbb{S}_{kB}^2$ 

- 1: **for**  $\forall S_i \in \mathbb{S}_{kB}^{1,2}$  **do**
- 2:     Calculate the *contact duration* between  $S_i$  and the  $UAV_1$  (denoted as  $T_{i,1}$ ), the  $UAV_2$  (denoted as  $T_{i,2}$ ), respectively;
- 3:     **if**  $T_{i,1} < T_{i,2}$  **then**
- 4:          $\mathbb{S}_{kB}^2 = \mathbb{S}_{kB}^2 \cup \{S_i\}$ ;
- 5:     **else**
- 6:          $\mathbb{S}_{kB}^1 = \mathbb{S}_{kB}^1 \cup \{S_i\}$ ;
- 7:     **end if**
- 8: **end for**
- 9: **return**  $\mathbb{S}_{kB}^1$  and  $\mathbb{S}_{kB}^2$ ;

**Table 3.** Proposed algorithms

Algorithms	Descriptions
Balance mechanism	It is specially used to balance the communications between multiple nodes and multiple UAVs for the system.
PCdFS mechanism	It is used to build the "scheduling" between the nodes (that only with the range of a single UAV) and the UAV.
PMCdFS mechanism	It is specially used to balance the communications between the nodes (these nodes are within the range of multiple UAVs at the same time) and the UAV.

**Table 4.** Simulation parameters

Parameter	Value	Parameter	Value
network size	[5, 200]	path width	10 <i>m</i>
fly time	5 <i>minutes</i>	fly height	[5, 95] <i>m</i>
UAV speed	[5, 25] <i>ms</i> <sup>-1</sup>	sensor speeds	[0, 10] <i>ms</i> <sup>-1</sup>
# priority groups	[2, 5]	packet size	127 <i>Bytes</i>
Data bit rate	250 <i>kbps</i>	inter-beacon duration	2 <i>second</i> to 60 <i>second</i>
receiving threshold	1E-10 <i>W</i>	sensing threshold	1E-11 <i>W</i>
transmission range of the UAV and the node	100 <i>m</i>		

**Table 5.** Summary of simulations.

Section	Parameters	$N_{uav}$	Descriptions
Section 5.1.1. Impact of priority level changes.	$N = 200, h = 15 \text{ m}, v = 10 \text{ ms}^{-1}, \text{IBD} = 2 \text{ s}, v_i \in [0,10] \text{ ms}^{-1}, N_{pl} \in \{2,3,4,5\}$ .	1	Study the impact of priority levels on the network performance.
Section 5.1.2. Varying beacon intervals.	$N = 200, h \in [5,95] \text{ m}, v \in [5,25] \text{ ms}^{-1}, \text{IBD} \in [2,60] \text{ s}, v_i \in [0,10] \text{ ms}^{-1}, N_{pl} = 2$ .	1	Study the impact of different synchronization frequency on the network performance.
Section 5.1.3. Impact of UAV's parameters changes.	$N = 200, h = 15 \text{ m}, v = 10 \text{ ms}^{-1}, \text{IBD} = 2 \text{ s}, v_i \in [0,10] \text{ ms}^{-1}, N_{pl} = 2$ .	1	Study the impact of fly height and speeds on the network performance.
Section 5.1.4. Scalability.	$N \in [5,200], h = 15 \text{ m}, v = 10 \text{ ms}^{-1}, \text{IBD} = 2 \text{ s}, v_i \in [0,10] \text{ ms}^{-1}, N_{pl} = 2$ .	1	Study the impact of the network size on the network performance.
Section 5.1.5. Comparison between Multi-UAVs and Single-UAV.	$N = 200, h = 15 \text{ m}, v = 10 \text{ ms}^{-1}, \text{IBD} = 2 \text{ s}, v_i \in [0,10] \text{ ms}^{-1}, N_{pl} = 2$ .	{1,2}	Compare our proposed algorithms when using one UAV and two UAVs.

## 278 5.1. Simulations

279 We conduct the simulations in MATLAB/Simulink where the UAV fly (5 minutes) along a path  
 280 (the path is 10 *m* wide). The simulated priority groups are {2, 3, 4, 5} groups. The other simulation  
 281 parameters are presented in table 4, the final results are given by the mean of 30 simulation runs.  
 282 Considering that, the PFS mechanism is proposed and examined based on a single-UAV sensor  
 283 network. To well compare the proposed algorithm with it, we use  $M = 1$  in the simulations in Section  
 284 5.1.1, Section 5.1.2, Section 5.1.3, and Section 5.1.4. And in Section 5.1.5, we compare our proposed  
 285 algorithms when using single UAV and multiple UAVs. All the simulations are summarized in Table 5.

### 286 5.1.1. Impact of priority level changes

287 Figure 6 presents the impact for varying the number of priority groups. The more priority groups,  
 288 the smaller number of collected packets. The number of collected packets is much improved at 2  
 289 priority groups division as compare to 5 priority groups division. That is because the nodes in lower  
 290 priority groups may have changed their state when it is their turn to send packets. The introduce of

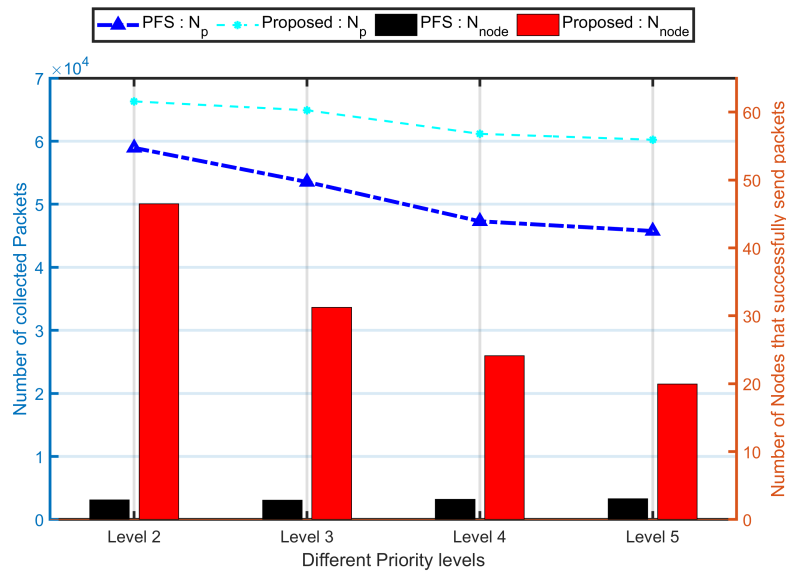


**Figure 6.** Impact of priority area change. In these simulations, the proposed algorithm is the combination of proposed Balance and PCdFS algorithms.

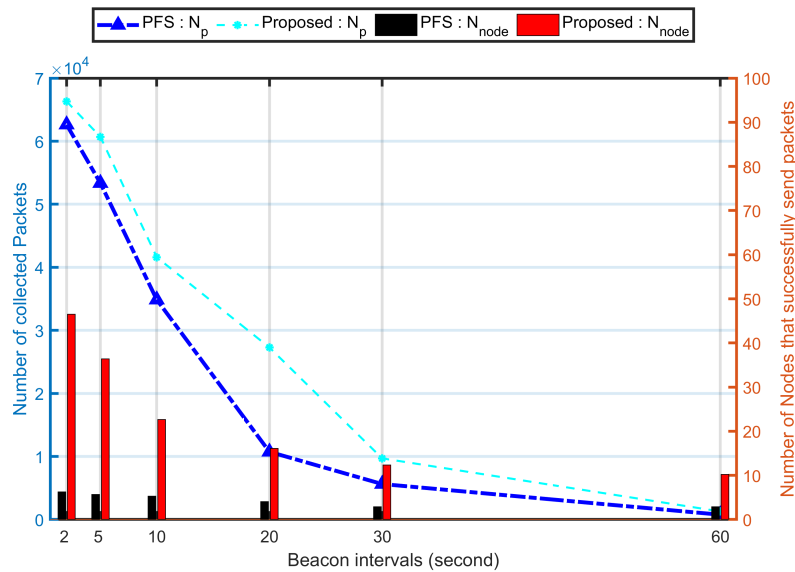


**Figure 7.** The impact of inter-beacon duration on network performance. In these simulations, the proposed algorithm is the combination of proposed Balance and PCdFS algorithms.

291 contact duration provides high priority to them so as to overcome part of this issue, thus more packets  
 292 were collected in PCdFS algorithm.

293 It also can be concluded that, the larger number of priority groups, the smaller number of nodes  
 294 are within the highest priority group. Then, the smaller number of nodes have opportunities to send  
 295 packets, thus, the unfair for the network. The number of nodes that successfully send at least one  
 296 packet in proposed Priority-based Contact-duration Frame Selection mechanism is **16.2** times larger  
 297 than in the PFS mechanism which is because the dynamic parameters are concerned in the proposed  
 298 algorithm.

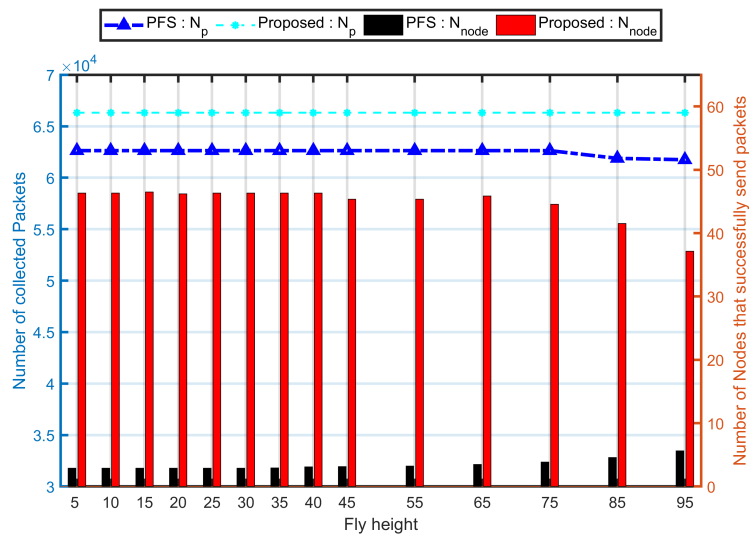
299 In the following, in both simulations and real experiments, the number of priority groups is fixed  
 300 at 2.

301 5.1.2. Varying beacon intervals

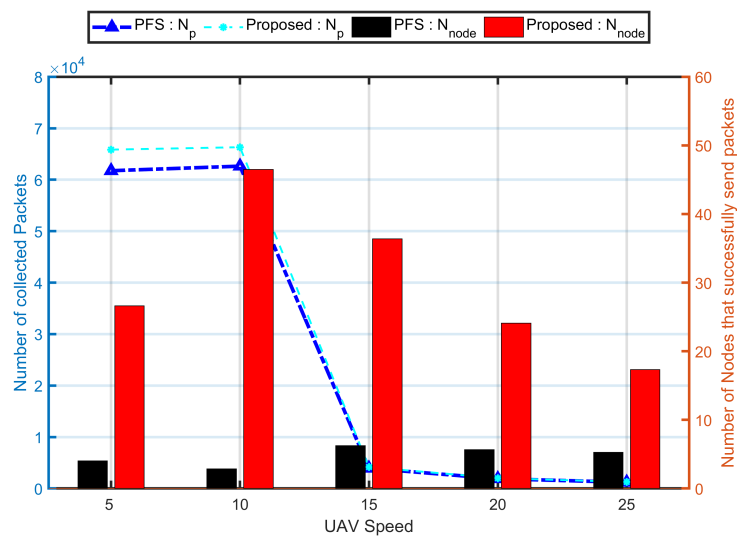
302 Figure 7 shows that both  $N_p$  and  $N_{node}$  were much improved when the inter-beacon duration at 2  
 303 seconds. Indeed, the longer the beacon intervals, the smaller number of beacons were sent. Thus, the  
 304 number of network synchronization is reduced so as to seldom nodes were detected during collecting.  
 305 No node will be detected if no beacon sending.

306 5.1.3. Impact of UAV's parameters changes

307 Figure 8 shows the impact of the total number of collected packets for varying the UAV speed and  
 308 fly height. The network achieve the optimal ( $N_{node} = 46.5$  of 30 simulations) when the fly height is 15  
 309 m (Figure 8(a)). In this simulation, the UAV speed is  $10\text{ ms}^{-1}$ , and the size is 200 with nodes speeds



(a) The number of collected packets for the network for varying fly height of the UAV. The number of nodes that successfully send packet to the UAV in the same scenario.



(b) The number of collected packets for the network for varying UAV' speed. The number of nodes that successfully send packet to the UAV for varying the speed of the UAV.

**Figure 8.** Network performance for varying UAV' parameters: fly height and speed. In these simulations, the proposed algorithm is the combination of proposed Balance and PCdFS algorithms.

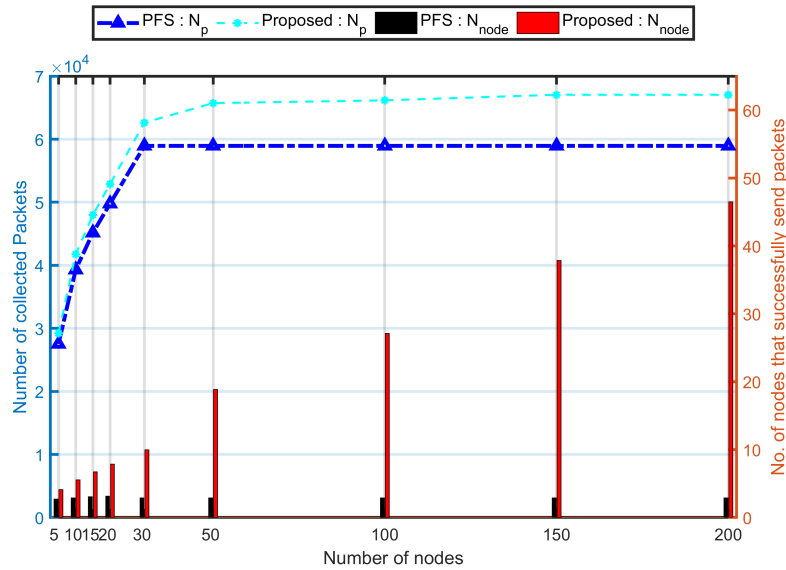


**Figure 9.** Evaluation of proposed algorithm (the combination of proposed Balance and PCdFS algorithms) on network size.

310 vary from  $1 \text{ ms}^{-1}$  to  $10 \text{ ms}^{-1}$ . Due to using fixed  $Dr$ , the fly height has very slight impact on both  
 311  $N_p$  and  $N_{node}$ . The contact duration which given by the relative distance between the nodes and the  
 312 UAV was highly affected by the fly height. Hence, the PCdFS algorithm presents difference from the  
 313 PFS mechanism when the fly height is  $95 \text{ m}$ . Compared to  $N_p$ , the  $N_{node}$  was affected much when the  
 314 fly height is larger than  $75 \text{ m}$ . There is clearly difference between the two mechanisms when the gap  
 315 between different fly heights exceeds  $50 \text{ m}$ .

316 The change of the UAV speed has huge impact on both the total number of collected packets and  
 317 the number of nodes that successfully send packets to the UAV 8(b). When the gap between the UAV  
 318 speed and the maxi speed of all nodes is very small, the network performance achieve the optimal.  
 319 In this studied scenario, the maxi speed for all nodes is  $10 \text{ ms}^{-1}$ , thus, the performance is optimal  
 320 when the UAV speed is  $10 \text{ ms}^{-1}$ . When  $V_{uav} > 10 \text{ ms}^{-1}$ , the higher the  $V_{uav}$ , the bigger gap between  
 321 the UAV speed and the nodes' speeds, the shorter contact duration between them, then, the smaller  
 322 opportunities for nodes to communicate with the UAV. Then, the smaller number of packets were send  
 323 to the UAV, the unfair for the network.

#### 324 5.1.4. Scalability

325 Figure 9 shows the impact of the network size on system performance. In this study, the fly height  
 326 is  $15 \text{ m}$  and UAV's speed is  $10 \text{ ms}^{-1}$  and the size vary from 5 to 200 with nodes' speeds vary from  
 327  $1 \text{ ms}^{-1}$  to  $10 \text{ ms}^{-1}$ .

328 The larger the network size, the larger number of nodes have opportunity to communicate with  
 329 the UAV, thus, the larger number of packets were sent to the UAV. When the size larger than 30, each  
 330 time-slots has successfully communication, thus, the number of collected packets in PFS mechanism  
 331 keep steady. It keep increase in PCdFS algorithm until it reach the transmission upper bound of the  
 332 collection time. The  $N_{node}$  was increase steady in proposed algorithm. The  $N_{node}$  when  $N = 200$   
 333 in proposed algorithm is 11.34 times larger than when  $N = 5$  while it is almost the same in PFS  
 334 mechanism. Hence, the proposed algorithm shows high scalability in terms of sensors density.

#### 335 5.1.5. Comparison between Multi-UAVs and Single-UAV

336 Figure 10 presents the impact of proposed algorithms on the network size. "Alg1/UAV<sub>1</sub>" simulate  
 337 the combination of proposed Balance and PCdFS algorithms on the UAV<sub>1</sub> which is take-off from

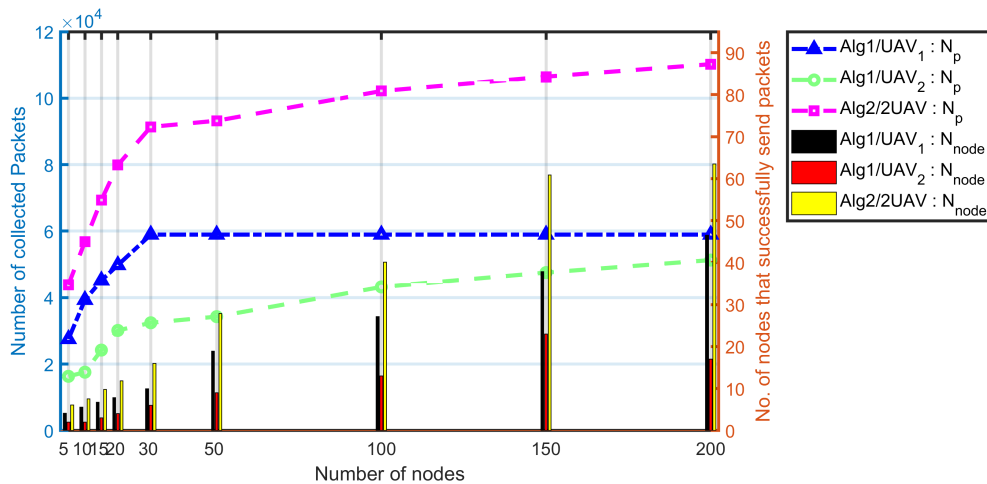


**Figure 10.** The impact of  $UAV_1$ ,  $UAV_2$  and multi-UAVs of proposed algorithm on network size. In these simulations, "Alg1" is the combination of proposed Balance and PCdFS algorithms, "Alg2" is the combination of proposed PMCdFS, PCdFS, and Balance algorithms.

338 the original point of the path, while "Alg1/ $UAV_2$ " simulate the same combination algorithms on the  
 339  $UAV_2$  which is take-off from the end point (the midline of the path) of the path.  $UAV_1$  fly at the same  
 340 direction as the nodes while  $UAV_2$  fly at opposite direction. Intuitively, the average contact duration  
 341 between the  $UAV_1$  and the nodes is longer than the average value between  $UAV_2$  and the nodes. Thus,  
 342 the communication conducted in  $UAV_1$  case work better than in  $UAV_2$ . There is no doubt that, the  
 343 multi-UAVs work better than single UAV in data collection issues because more opportunity provided  
 344 for mobile nodes.

## 345 5.2. Real Experiment

### 346 5.2.1. Set up

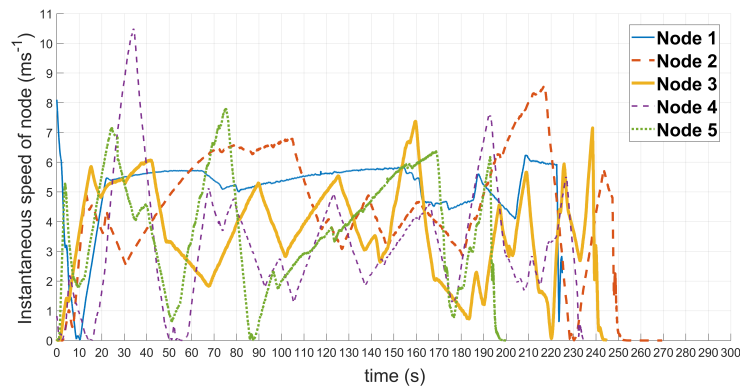
347 We study a path in Tongji University (Jiading Campus) as in Figure 11(a). It is 5 meters wide and  
 348 1200 meters long, with several intersections and 1 island (Figure 11(a)). In these experiments, the UAV  
 349 equips a Pixhawk autopilot system [42,43] (as shown in Figure 11(b)) so as to fly along a predefined  
 350 path at given height. The UAV controlled through a ground station (Figure 12) where the fly height  
 351 and speed and the packet transmission are controlled. We implement 15 bicycles move along the path  
 352 with each equips a Pixhawk to simulate the communications based on proposed algorithms (Figure



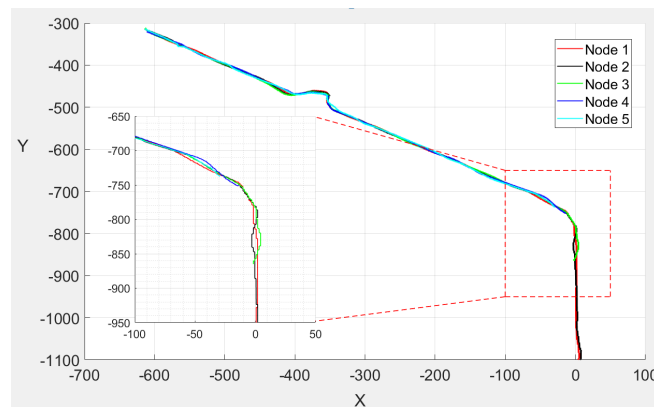
(a) Experiments path in Tongji University - Jiading Campus. (b) The UAV employed with a Pixhawk autopilot system. (c) The Pixhawk autopilot system deployed on a bicycle.

**Figure 11.** Presentation of the studied path and hardware in experiments.





(a) Instantaneous speeds of five nodes over time.



(b) Trajectories of five nodes.

**Figure 14.** The movements for 5 nodes.

353 11(c)). These nodes start with a random distance from the original point (point A in Figure 11(a)). Their  
 354 locations and speeds are expressed in NED coordinate system, as presented in Figure 11(a).

355 Pixhawk has built-in MAVLINK protocol [44], the protocol No.24 (GPS\_RAW\_INT) [44] is used  
 356 as the "beacon" packet (including the speed and location of the UAV) for the UAV, whose interval can  
 357 be configured (e.g., in the following experiments, the beacon intervals is set at 2 s). For mobile nodes,  
 358 the protocol No.24 (GPS\_RAW\_INT) is used as the "update" packet (including the speed and location  
 359 of the mobile node). We modified and reused the protocol NO.36 (SERVO\_OUTPUT\_RAW) [44] as the  
 360 "scheduling" packet (which stores the sensor ID and time-slot ID for the collision-free communication  
 361 between nodes and the UAV) for the UAV. Each MAVLINK packet contains a system ID field so we  
 362 can use it to identify the sender. The pixhawk has also a log system so the GPS information as well as  
 363 the received packet number and time is stored in the on-board SD card.

364 Figure 13 presents the movements for  $UAV_1$  (only one UAV is used in real experiments) where the  
 365 fly height is 15 meters, with control speeds of  $5 \text{ ms}^{-1}$  (Figure 13(a)) and  $3 \text{ ms}^{-1}$  (Figure 13(b)) according  
 366 to Pixhawk. In the studied experiments, the UAV fly at 15 m and 30 m. Figure 14 is an example to  
 367 present the instantaneous speeds and trajectories for 5 nodes (Node 1 to Node 5) according to the  
 368 Pixhawk.

369 To make the UAV fly along this path, we set 4 way points along the path as shown in Figure 12.  
 370 In the experiments, the UAV start from  $Point_1$  to achieve its given speed (it is  $5 \text{ ms}^{-1}$  in Figure 12) to  
 371  $Point_2$ ,  $Point_3$  and the ending point ( $Point_4$ ). In Pixhawk autopilot system, the UAV will hover on the  
 372 way point and ending point for 2 seconds. That is why in the Figure 13(a), the UAV speed is lower  
 373 than  $5 \text{ ms}^{-1}$  at  $P_2$  and  $P_3$ . In Figure 13(b), both the height and instantaneous speed of UAV have shock  
 374 between the  $Point_3$  and  $Point_4$  because of the influence of wind. The wind has impact on the dynamic

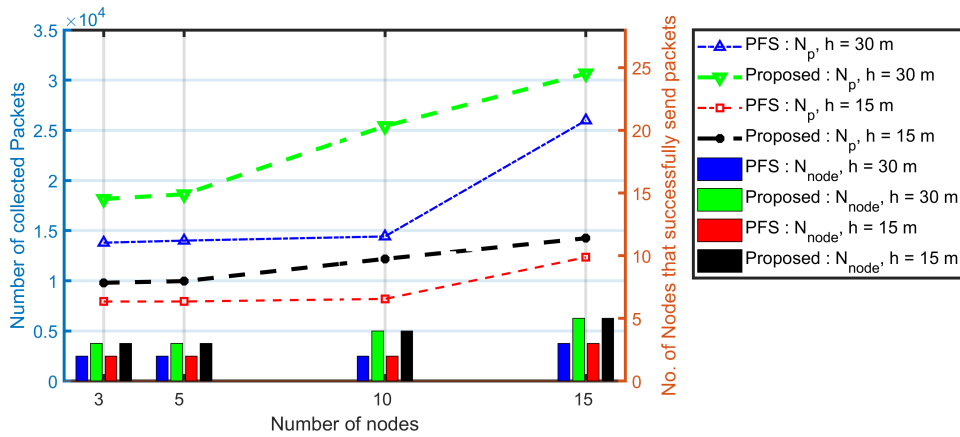


**Figure 15.** The impact of network size, and flying height over the system performance. In these experiments, the beacon interval is fixed at 2 seconds according to the simulation results in Figure 7.

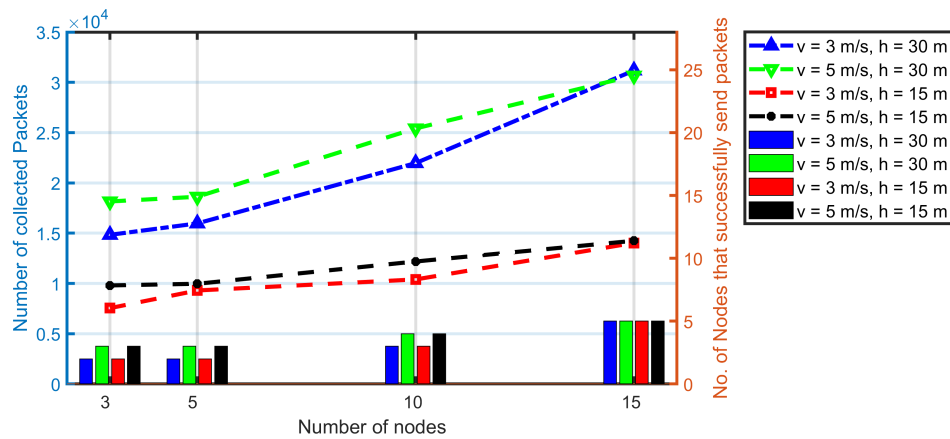


**Figure 16.** The impact of network size, and UAV's speed over the system performance. In these experiments, the beacon interval is fixed at 2 seconds. All the results are based on the combination of Balance and PCdFS algorithms.

375 parameters so as to affect the relative velocity between the mobile node and the UAV, the network  
 376 performance affected accordingly. However, it cannot be control during experiments.

### 377 5.2.2. Results

378 Figure 15 and Figure 16 show the experiments results under the proposed algorithms, the  
 379 combination of *Balance algorithm* and *PCdFS algorithm*. From Figure 15, the number of collected packets  
 380 in simulation is almost 2 times larger than in the experiments because of the impacts of hardware and  
 381 environments are not considered in simulations. The flying height has an significant impact on the  
 382 number of collected packets in experiments, especially when  $N_{node}$  is steady between different heights.  
 383 The higher the height, the larger number of nodes in both PFS and proposed algorithms. The number  
 384 of collected packets of proposed algorithm in size 15,  $h = 30$  meters is more than 2 times than in  $h = 15$   
 385 meters. The system performance increase as the size increase. The larger the network, the more nodes  
 386 have opportunities to send packets, the more packets were collected. The number of collected packets  
 387 in proposed algorithm (when  $h$  is 15 meters) is 1.2 times larger than in PFS algorithm.

388 From Figure 16, it can be found that the UAV's speed has little impact on data collection in real  
 389 experiments. This is because, the UAV's speed is set at  $3 \text{ ms}^{-1}$  and  $5 \text{ ms}^{-1}$  because of the battery  
 390 constrictions and the campus constrictions. And the nodes' speeds are between  $2 \text{ ms}^{-1}$  and  $5 \text{ ms}^{-1}$   
 391 also (Figure 14). Thus, the relative velocity between the UAV and mobile nodes are very small. The

392 number of collected packets presented in Figure 16 keep the same conclusions as in simulations in  
393 section 5.1.3 where the UAV fly at  $5\text{ ms}^{-1}$  and  $10\text{ ms}^{-1}$ .

394 The fly height almost have no influence on the number of nodes that successfully transmit packets  
395 to the UAV, as presented in both Figure 15 and Figure 16, which are the same as in section 5.1.3.

### 396 5.3. Discussions

397 According to the aforementioned simulations, the beacon interval and the UAV speed have huge  
398 impact on the network performance. The shorter the beacon interval, the better the system performance.  
399 The UAV speed is constrained by the node speed. The smaller the relative velocity between them,  
400 the higher the network performance. It keeps the same conclusions as in real experiment. In real  
401 experiments, the data collection is well conducted when the UAV speed is set at  $5\text{ ms}^{-1}$  which is very  
402 close to the average speed of mobile nodes. Compare to the other dynamic parameters, the number of  
403 priority levels has steady impact on data collection in the simulations. From the movements of the  
404 nodes in Figure 14, it can be found that, the difference between the trajectories of nodes are very small  
405 because the road width is  $5\text{ m}$  and the road length is  $1200\text{ m}$ .

406 Compare Figure 13(a) and Figure 13(b), it also can be found that, the fly time in  $3\text{ ms}^{-1}$  is 1.56  
407 times as in  $5\text{ ms}^{-1}$  while the speed increase by 66.67% (from  $3\text{ ms}^{-1}$  to  $5\text{ ms}^{-1}$ ). In the studied scenario,  
408 there are very small difference between the trajectories when UAV fly at  $3\text{ ms}^{-1}$  and  $5\text{ ms}^{-1}$  because  
409 the UAV follow the same path which width is very short compared to its length. Thus, the fly time is  
410 mainly dependent by the speed of the UAV. In other words, the slower the UAV fly, the higher energy  
411 consumption of the battery energy. From Figure 16, we notice that, the data collection has very little  
412 difference when UAV fly at  $3\text{ ms}^{-1}$  and  $5\text{ ms}^{-1}$ . Therefore, under given constrictions, the higher the fly  
413 speed of the UAV, the more saved battery energy.

414 The fly height has very little impact on data collection in simulations because of the same  
415 transmission rate is adopted. However, the fly height has huge impact on data collection in experiments  
416 because a real and complex antenna system are conducted among the transmissions between the node  
417 and the UAV. The higher the flying height, the less interference from external factors (e.g., buildings,  
418 etc.). Thus, the better the transmission, the higher the network performance.

## 419 6. Conclusion

420 In this paper, we developed two mechanisms: Priority-based Contact-duration Frame Selection  
421 mechanism (named PCdFS mechanism) and Priority-based Multiple Contact-duration Frame Selection  
422 mechanism (named PMCdFS mechanism). PCdFS mechanism is used to build the scheduling  
423 communications when the nodes are only covered by one of the UAVs. PMCdFS is used to balance the  
424 communication between the nodes and multi-UAVs when these node within the range of multi-UAVs  
425 at the same time. Based on the two mechanisms, we proposed the *Balance algorithm* which highly  
426 enhances the network fairness in the applications where both the nodes and the collectors are mobile.  
427 Two key mechanisms for designing *Balance algorithm* are: (i) divide the interesting areas into different  
428 priority areas and (ii) provide an independent priority value for each node in the same priority  
429 group according to their contact duration with the UAVs. We examined the performance of proposed  
430 algorithms through extensive simulations, and real experiments. In the experiments, we used 15  
431 mobile nodes at a path with several intersections and 1 island in Tongji campus in Shanghai, China. We  
432 also confirm the applicability of the proposed algorithm in a challenging and realistic scenario through  
433 numerous experiments. Both simulation results and experiment results present that the proposed  
434 PCdFS algorithm enhanced the network performance efficiently. The backhaul dimensioning is an  
435 interesting problem that we will address in our future work. It depends on the used backhaul type  
436 (either satellite or terrestrial) and on the allocation that is reserved to the network slice dedicated for  
437 MTC (Machine Type Communication) traffic.

**References**

- 439 1. Ali, F. UAV-enabled healthcare architecture: Issues and challenges. *Future generation computer systems* **2019**,  
440 97, 425–432.
- 441 2. Liu, X.; Ansari, N. Resource Allocation in UAV-Assisted M2M Communications for Disaster Rescue. *IEEE*  
442 *Wireless Communications Letters* **2019**, 8, 580–583.
- 443 3. Samir Labib, N.; Danoy, G.M.J.B.M.B.P. Internet of Unmanned Aerial Vehicles-A Multilayer Low-Altitude  
444 Airspace Model for Distributed UAV Traffic Management. *Sensors* **2019**, 19, 4779.
- 445 4. Mozaffari, M.; Saad, W.; Bennis, M.; Nam, Y.; Debbah, M. A Tutorial on UAVs for Wireless Networks:  
446 Applications, Challenges, and Open Problems. *IEEE Communications Surveys Tutorials* **2019**, 21, 2334–2360.
- 447 5. Poudel, S.; Moh, S. Medium Access Control Protocols for Unmanned Aerial Vehicle-Aided Wireless Sensor  
448 Networks: A Survey. *IEEE Access* **2019**, 7, 65728–65744.
- 449 6. Samir, M.; Sharafeddine, S.; Assi, C.M.; Nguyen, T.M.; Ghrayeb, A. UAV Trajectory Planning for Data  
450 Collection from Time-Constrained IoT Devices. *IEEE Transactions on Wireless Communications* **2020**, 19, 34–46.
- 451 7. Liu, J.; Wang, X.; Bai, B.; Dai, H. Age-optimal trajectory planning for UAV-assisted data collection. *2018 IEEE*  
452 *INFOCOM - IEEE Conference on Computer Communications Workshops (INFOCOM WKSHPS)*, Honolulu, HI,  
453 **2018**. pp. 553–558.
- 454 8. Tong, P.; Liu, J.; Wang, X.; Bai, B.; Dai, H. UAV-Enabled Age-Optimal Data Collection in Wireless Sensor  
455 Networks. *2019 IEEE International Conference on Communications Workshops (ICC Workshops)*, Shanghai, China,  
456 **2019**. pp. 1–6.
- 457 9. Mario.; Di.; Francesco.; Sajal.; K.; Das.; Giuseppe.; Anastasi. Data Collection in Wireless Sensor Networks  
458 with Mobile Elements: A Survey. *ACM transactions on sensor networks* **2011**, 8(1), 7.1–7.31.
- 459 10. Zhao, M.; Ma, M.; Yang, Y. Efficient Data Gathering with Mobile Collectors and Space-Division Multiple  
460 Access Technique in Wireless Sensor Networks. *IEEE Transactions on Computers* **2011**, 60, 400–417.
- 461 11. Pang, Y.; Zhang, Y.; Gu, Y.; Pan, M.; Han, Z.; Li, P. Efficient data collection for wireless rechargeable sensor  
462 clusters in Harsh terrains using UAVs. *2014 IEEE Global Communications Conference*, Austin, TX, **2014**, pp.  
463 234–239.
- 464 12. Ma, X.; Kacimi, R.; Dhaou, R. Fairness-aware UAV-assisted data collection in mobile wireless sensor  
465 networks. *2016 International Wireless Communications and Mobile Computing Conference (IWCMC)*, Paphos,  
466 Cyprus, **2016**, pp. 995–1001.
- 467 13. MA, X. Data Collection of Mobile Sensor Networks by Drones. [Online Available, 2017.12]:  
468 <http://docplayer.fr/18339015-These-en-vue-de-l-obtention-du-doctorat-de-l-universite-detoulouse.html> **2017**.
- 469 14. Ho, D.; Park, J.; Shimamoto, S. Performance evaluation of the PFSC based MAC protocol for WSN employing  
470 UAV in rician fading. *2011 IEEE Wireless Communications and Networking Conference*, Cancun, Quintana Roo,  
471 **2011**. pp. 55–60.
- 472 15. Ho, D.; Shimamoto, S. Highly reliable communication protocol for WSN-UAV system employing TDMA  
473 and PFS scheme. *2011 IEEE GLOBECOM Workshops (GC Wkshps)*, Houston, TX, **2011**. pp. 1320–1324.
- 474 16. Ma, X.; Chisiu, S.; Kacimi, R.; Dhaou, R. Opportunistic communications in WSN using UAV. *2017 IEEE*  
475 *Annual Consumer Communications and Networking Conference (CCNC)*, Las Vegas, NV, **2017**. pp. 510–515.
- 476 17. F. D. Alterio, L. Ferranti, L. Bonati, F. Cuomo and T. Melodia. Quality Aware Aerial-to-Ground 5G Cells  
477 through Open-Source Software. *2019 IEEE Global Communications Conference (GLOBECOM)*, Waikoloa, HI,  
478 USA, **2019**, pp. 1-6.
- 479 18. Raveneau P , Chaput E , Dhaou R , et al. Carreau: CARrier REsource access for mUle, DTN applied to hybrid  
480 WSN / satellite system. *2013 IEEE Vehicular Technology Conference (VTC Fall)*. Las Vegas, NV, **2013**, pp. 1-5.
- 481 19. P. Raveneau, E. Chaput, R. Dhaou, E. Dubois, P. Gelard and A. Beylot. Martinet: A disciplinarian protocol  
482 for resource access in DTN. *2013 IFIP Wireless Days (WD)*, Valencia, **2013**, pp. 1-3.
- 483 20. Zhan, C.; Zeng, Y. Completion Time Minimization for Multi-UAV-Enabled Data Collection. *IEEE Transactions*  
484 *on Wireless Communications* **2019**, 18, 4859–4872.
- 485 21. Shen, C.; Chang, T.; Gong, J.; Zeng, Y.; Zhang, R. Multi-UAV Interference Coordination via Joint Trajectory  
486 and Power Control. *IEEE Transactions on Signal Processing* **2020**, 68, 843–858.
- 487 22. Ebrahimi, D.; Sharafeddine, S.; Ho, P.; Assi, C. UAV-Aided Projection-Based Compressive Data Gathering in  
488 Wireless Sensor Networks. *IEEE Internet of Things Journal* **2019**, 6, 1893–1905.

- 489 23. Zhan, C.; Huang, R. Energy Minimization for Data Collection in Wireless Sensor Networks with UAV. *2019*  
490 *IEEE Global Communications Conference, Waikoloa, HI, 2019*. pp. 1–6.
- 491 24. Zhan, C.; Lai, H. Energy Minimization in Internet-of-Things System Based on Rotary-Wing UAV. *IEEE*  
492 *Wireless Communications Letters* **2019**, *8*, 1341–1344.
- 493 25. Gong, J.; Chang, T.; Shen, C.; Chen, X. Flight Time Minimization of UAV for Data Collection Over Wireless  
494 Sensor Networks. *IEEE Journal on Selected Areas in Communications* **2018**, *36*, 1942–1954.
- 495 26. Zong, J.; Shen, C.; Cheng, J.; Gong, J.; Chang, T.; Chen, L.; Ai, B. Flight Time Minimization via UAV's  
496 Trajectory Design for Ground Sensor Data Collection. *2019 International Symposium on Wireless Communication*  
497 *Systems (ISWCS), Oulu, Finland, 2019*. pp. 255–259.
- 498 27. Popescu, D.; Stoican, F.S.G.C.O.I.L. A Survey of Collaborative UAV-WSN Systems for Efficient Monitoring.  
499 *Sensors* **2019**, *19*, 4690.
- 500 28. Lin, H.; Yan, Z.; Chen, Y.; Zhang, L. A Survey on Network Security-Related Data Collection Technologies.  
501 *IEEE Access* **2018**, *6*, 18345–18365.
- 502 29. Jing, X.; Yan, Z.; Pedrycz, W. Security Data Collection and Data Analytics in the Internet: A Survey. *IEEE*  
503 *Communications Surveys Tutorials* **2019**, *21*, 586–618.
- 504 30. Li, J.; Zhao, H.; Wang, H.; Gu, F.; Wei, J.; Yin, H.; Ren, B. Joint Optimization on Trajectory, Altitude, Velocity,  
505 and Link Scheduling for Minimum Mission Time in UAV-Aided Data Collection. *IEEE Internet of Things*  
506 *Journal* **2020**, *7*, 1464–1475.
- 507 31. Wang, Z.; Liu, R.; Liu, Q.; Thompson, J.S.; Kadoch, M. Energy-Efficient Data Collection and Device  
508 Positioning in UAV-Assisted IoT. *IEEE Internet of Things Journal* **2020**, *7*, 1122–1139.
- 509 32. You, C.; Zhang, R. 3D Trajectory Optimization in Rician Fading for UAV-Enabled Data Harvesting. *IEEE*  
510 *Transactions on Wireless Communications* **2019**, *18*, 3192–3207.
- 511 33. Hu, Q.; Cai, Y.; Yu, G.; Qin, Z.; Zhao, M.; Li, G.Y. Joint Offloading and Trajectory Design for UAV-Enabled  
512 Mobile Edge Computing Systems. *IEEE Internet of Things Journal* **2019**, *6*, 1879–1892.
- 513 34. Hu, Y.; Yuan, X.; Xu, J.; Schmeink, A. Optimal 1D Trajectory Design for UAV-Enabled Multiuser Wireless  
514 Power Transfer. *IEEE Transactions on Communications* **2019**, *67*, 5674–5688.
- 515 35. Qin, Z.; Dong, C.W.H.L.A.D.H.S.W.X.Z. Trajectory Planning for Data Collection of Energy-Constrained  
516 Heterogeneous UAVs. *Sensors* **2019**, *19*, 4884.
- 517 36. Alessandro, R. A Risk-Aware Path Planning Strategy for UAVs in Urban Environments. *Journal of Intelligent*  
518 *and Robotic Systems* **2018**, pp. 629–643.
- 519 37. Zeng, Y.; Xu, X.; Zhang, R. Trajectory Design for Completion Time Minimization in UAV-Enabled  
520 Multicasting. *IEEE Transactions on Wireless Communications* **2018**, *17*, 2233–2246.
- 521 38. Wu, Q.; Zeng, Y.; Zhang, R. Joint Trajectory and Communication Design for Multi-UAV Enabled Wireless  
522 Networks. *IEEE Transactions on Wireless Communications* **2018**, *17*, 2109–2121.
- 523 39. Luitpold, B. Coordinated Target Assignment and UAV Path Planning with Timing Constraints. *Journal of*  
524 *Intelligent and Robotic Systems* **2019**, pp. 857–869.
- 525 40. Hu, J.; Zhang, H.; Song, L. Reinforcement Learning for Decentralized Trajectory Design in Cellular UAV  
526 Networks With Sense-and-Send Protocol. *IEEE Internet of Things Journal* **2019**, *6*, 6177–6189.
- 527 41. Liu, Y.; Gao, C.; Zhang, Z.; Lu, Y.; Chen, S.; Liang, M.; Tao, L. Solving NP-Hard Problems with  
528 Physarum-Based Ant Colony System. *IEEE/ACM Transactions on Computational Biology and Bioinformatics*  
529 **2017**, *14*, 108–120.
- 530 42. Lesko, J.; Schreiner, M.; Megyesi, D.; Kovacs, L. Pixhawk PX-4 Autopilot in Control of a Small Unmanned  
531 Airplane. *2019 Modern Safety Technologies in Transportation (MOSATT), Kosice, Slovakia, 2019*. pp. 90–93.
- 532 43. PixhawkWeb (built on: 2013.07). <https://pixhawk.org/>.
- 533 44. MAVLINK (built on: 2015.10). <https://mavlink.io/en/messages/common.html>.